

The Influence of Sodium Silicate Concentration and Impregnation Time on Biochar Activation for Water Adsorption

Hadiantono Hadiantono^a, Mohamad Djaeni^{a,*}, Indro Sumantri^a, Suherman Suherman^a, Hadiyanto Hadiyanto^a, Nandang Mufti^b

^aDepartment of Chemical Engineering, Faculty of Engineering, Diponegoro University. Jl. Prof. H. Soedarto SH, Tembalang, Semarang 50275, Central Java, Indonesia

^bDepartment of Physics, Faculty of Mathematics and Science, State University of Malang, Jl. Semarang No. 5, Sumbersari, Lowokwaru, Malang 65145, East Java, Indonesia
moh.djaeni@live.undip.ac.id

A composite desiccant for water vapor adsorption, based on biomass-derived activated carbon (biochar) impregnated with sodium silicate, is presented. Silica gel is introduced into the biochar pores to enhance the water vapor adsorption capacity. Characterization using nitrogen isothermal adsorption, SEM imaging, and Fourier Transform Infrared (FTIR) analysis reveals that impregnation decreases the specific surface area and pore volume while increasing the concentration and types of oxygen-containing functional groups on the surface. The water vapor adsorption analysis demonstrates that the composite, under optimal conditions (20 wt% Na₂SiO₃ and 60 hours of impregnation), exhibits an equilibrium adsorption capacity quadruple that of non-impregnated biochar. Nevertheless, exceeding the optimal Na₂SiO₃ concentration or impregnation duration diminishes adsorption capacity. Kinetic analysis employing pseudo-first-order (PFO) and pseudo-second-order (PSO) models revealed that non-impregnated biochar fitted both models almost equally, whereas Na₂SiO₃-impregnated biochar followed the PSO model, as evidenced by higher R² values.

1. Introduction

Humidity control is essential for human comfort, industry, pharmaceuticals, and food processing. Electronics manufacturing also requires low humidity (40 – 50% RH) for high precision. In tropical regions like Indonesia, humidity averages around 70%, greatly beyond the recommended range of 40 – 60% for human health, leading to discomfort and health issues (Wolkoff, 2018). Air dehumidification improves thermal comfort and supports industrial growth. Traditional cooling methods are inefficient as they require reheating air after over-cooling to the dew point, consuming 20% of the system energy. Various industrial dehumidification techniques, particularly fluidized bed, condensation, fixed bed, and rotating wheel systems have drawbacks, including high energy consumption and heat generation during adsorption. Integrating solid desiccants into heat exchangers can increase efficiency by managing both sensible and latent (Wang et al., 2022).

In food processing, dehumidification is necessary for drying, which extends shelf life. However, the sun drying method, which is commonly used in developing countries, experiences challenges like pests and weather. Artificial drying methods are energy-intensive and costly, contributing to carbon emissions. Adsorption drying with desiccants offers a more efficient option, reducing drying time, energy consumption, and color retention. Desiccants help by absorbing moisture from the air, lowering relative humidity, and thereby increasing the moisture transfer rate from food to the air. This method shortens drying time, saves energy, and enhances color retention compared to conventional heating techniques (A'yuni et al., 2021; Asiah et al., 2017).

Various adsorbents have been investigated for use as desiccants, including carbon material, silica gel, silica gel composites, zeolite, polyvinyl alcohol composites, and metal-organic frameworks (MOF) (Wang et al., 2022). However, each material has limitations, particularly silica gel's low thermal conductivity, the low adsorption capacity of powdered zeolites, the low density of carbon materials, and the high preparation costs of polymers and MOFs (Vivekh et al., 2020). Activated carbon (AC) is a proven adsorbent, known for its high porosity, non-

toxicity, and thermal stability. It can be derived from coal or biomass, which have a high carbon content and low inorganic components. Biomass, being renewable and abundant, is a particularly attractive precursor. However, AC is a hydrophobic and low-density material, therefore, surface modification is required for water vapor adsorption. Impregnating the carbon with silica (Na_2SiO_3) can enhance its hydrophilicity (Wang et al., 2022). Despite numerous studies on biomass-derived AC, there is limited research on water vapor adsorption under specific ambient conditions. Thus, this study aims to develop a Na_2SiO_3 -impregnated AC composite adsorbent.

2. Materials and methods

The following reagents and materials were used in this work: Rice husk char (RHAC) (South Tangerang, Banten, Indonesia); mangrove wood char (MWAC) (East Jakarta, Jakarta, Indonesia); coconut shell char (CSAC) (East Jakarta, Jakarta, Indonesia); sodium silicate (Na_2SiO_3) (water content of 47.17%, ROFA Laboratorium Centre Ltd. Co., Indonesia); HCl (concentration of 32%, ROFA Laboratorium Centre Ltd. Co., Indonesia); distilled water. Figure 1 shows the preparation process of biochar based composite desiccant. The dried and sieved to 20 and 25 mesh AC (5 g) was added to 100 ml of Na_2SiO_3 solution (5, 9, 13, 17, 20, 24, 27%wt) with stirring using magnetic stirrer before being stored at room temperature (for 12, 24, 36, 48, 60, 72 h). The impregnated AC was rinsed using distilled water and 5 %v HCl until the pH reached neutral, then dried at 120°C overnight.

The ultimate analysis was performed using a Thermo Scientific FlashSmart Elemental (CHNS/O) Analyzer to quantify C, H, N, S, and O content. A scanning electron microscope (SEM, FEI, Inspect-S50) equipped with Energy-Dispersive X-ray Spectroscopy (EDX) was used to examine morphological changes and elemental composition. The specific surface area was determined through N_2 adsorption-desorption isotherms at -196 °C using a Micromeritics Tristar II Plus 3020, with the BET equation for specific surface area (SSA) calculation and BJH method for average pore size analysis. Fourier Transform Infrared (FTIR) spectroscopy (Shimadzu, IRPrestige 21) characterized surface functional groups before and after impregnation.

The adsorption capacity of the AC was evaluated by placing 3g of AC in an isolated glass jar filled with pure water for about 20% of the jar capacity. Under this condition, the average relative humidity (RH) of the system is 96.88%. The evaluation was conducted at room temperature (average of 29.81 °C) by measuring the weight change every 24 hours until a constant weight was achieved. The adsorption kinetics were evaluated using the pseudo-first-order (PFO) and pseudo-second-order (PSO) models (Jia et al., 2025) (Table 1.).



Figure 1. The preparation process and experimental setup of biochar based composite desiccant

Table 1: Kinetic models used in this study

Model	Non-linear form	Linear form
Pseudo-first-order	$\frac{dq_t}{dt} = k_1(q_e - q_t)$	$\ln(q_e - q_t) = -k_1t + \ln q_e$
Pseudo-second-order	$\frac{dq_t}{dt} = k_2(q_e - q_t)^2$	$\frac{t}{q_t} = \frac{1}{k_2q_e^2} + \frac{t}{q_e}$

Where q_e : equilibrium adsorption capacity (g/g), q_t : adsorption capacity at time t (g/g), k_1 : PFO rate constant (day^{-1}), k_2 PSO rate constant (g/g/day), t : adsorption time (day)

3. Results and Discussion

The ultimate analysis results indicate that RHAC and CSAC have high carbon content, whereas MWAC has significantly lower carbon content (Table 2). According to Mongkito et al. (2020), carbonization at higher temperatures increases carbon content by promoting poly-aromatic structure formation. The low carbon content in MWAC suggests sub-optimal carbonization compared to RHAC and CSAC. The absence of nitrogen (N) in all samples indicates low nitrogen content in the raw materials, as nitrogen molecules volatilize during carbonization. MWAC contains 2.52% sulfur (S), whereas RHAC and CSAC have none, which is attributed to the mangrove habitat where sulfur-rich sediments facilitate sulfur absorption into the wood. The lower oxygen content in RHAC and CSAC suggests higher carbonization temperatures than MWAC, reducing polar functional groups and increasing hydrophobicity (Lee et al., 2019). Figure 2 illustrates the morphological differences between MWAC and MWAC/Si-20%,60h. The MWAC surface exhibits an irregular structure with a complex

network of pores and channels (Figure 2(a)), formed due to the release of volatile compounds during carbonization. After Na_2SiO_3 impregnation for 60 hours, significant structural modifications occur, leading to more developed and evenly distributed pores (Figure 2(b)). The impregnation by Na_2SiO_3 follows the reaction as in Equation 1 (Guo & Wang, 2023), where the NaOH formed infiltrates the carbon framework, enhancing porosity. However, some pores become blocked by silica gel due to impregnation (Wang et al., 2022).

Table 2: Results of ultimate analysis on different biochars

Sample	Element (%)				
	C	H	N	S	O
MWAC	25.0702	2.7372	-	2.5240	2.4069
RHAC	54.6369	2.8297	-	-	1.8360
CSAC	62.4755	4.5260	-	-	1.8763



Figure 2(c–d) depicts a decrease in carbon content from 79.06% (MWAC) to 67.37% (MWAC/Si-20%,60h), attributed to carbon surface reactions with NaOH (Eq. 2).



The Na^+ ions produced during impregnation may occupy vacant sites and replace functional groups on the activated carbon surface, explaining the increase in Na content from 0.38% to 3.25%. The oxygen percentage increased from 20.37% to 28.29%, indicating hydroxide ions (OH^-) reacting with carbon atoms to form new surface functional groups (Li et al., 2020). The presence of silica in MWAC/Si-20%,60h was confirmed by EDX spectra, showing a Si content of 0.70% (Figure 2(d)).

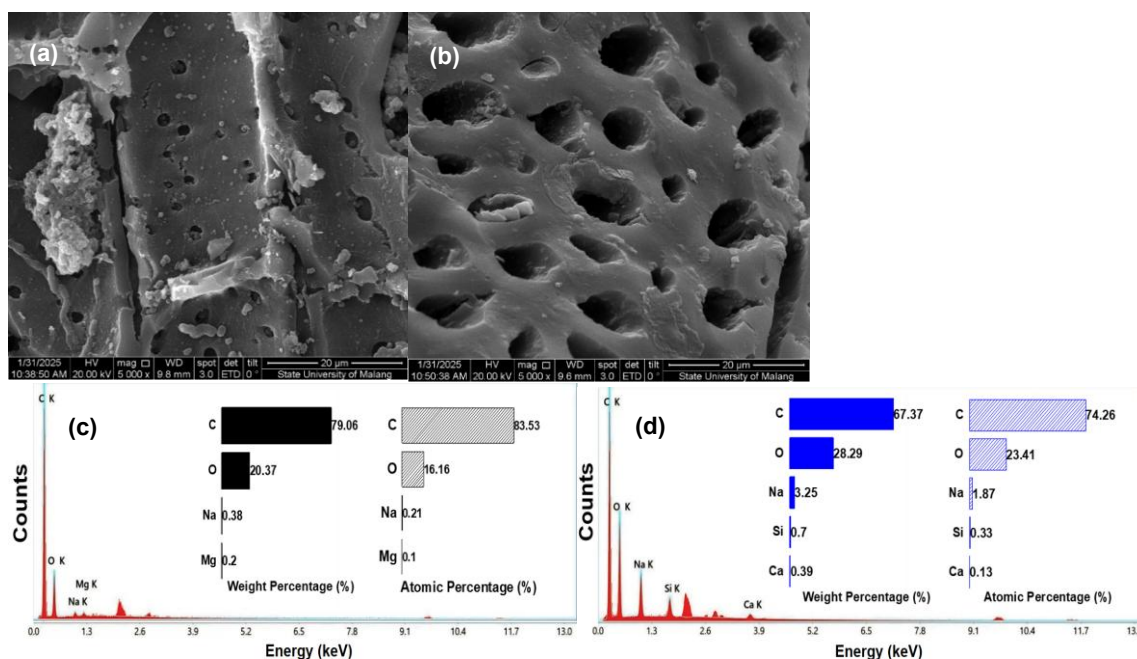


Figure 2: SEM images of (a) MWAC and (b) MWAC/Si-20%,60h with element content of (c) MWAC and (d) MWAC/Si-20%,60h

Figure 3(a) presents the N_2 adsorption isotherms. MWAC and MWAC/Si-20%,60h exhibit Type II isotherms, indicating the presence of macropores. The significant increase in adsorption at high P/P_0 in MWAC confirms progressive macropore filling. MWAC/Si-20%,60h shows reduced surface area after silica impregnation due to pore blockage. In contrast, RHAC and CSAC exhibit Type IV isotherms with clear hysteresis loops, characteristic of mesoporous materials (Thommes et al., 2015). MWAC/Si-20%,60h has a significantly larger pore size than other samples due to NaOH reaction with MWAC's surface. Figure 3(b) presents the FTIR spectra of MWAC and its composite. The broad peak at $\sim 3265 \text{ cm}^{-1}$ corresponds to hydroxyl ($-\text{OH}$) stretching, with MWAC/Si-20%,60h displaying higher intensity due to silanol ($\text{Si}-\text{OH}$) formation. The absorption band at $\sim 2933 \text{ cm}^{-1}$ represents C–H stretching, while the peak at $\sim 1620 \text{ cm}^{-1}$ is attributed to C=O stretching. The band at ~ 1230

cm^{-1} corresponds to C–O stretching (Nandiyanto et al., 2019). MWAC/Si-20%,60h shows a slight intensity increase at $\sim 1033 \text{ cm}^{-1}$, indicating Si–O–Si bonding, confirming Si incorporation from Na_2SiO_3 impregnation (Cuong et al., 2020).

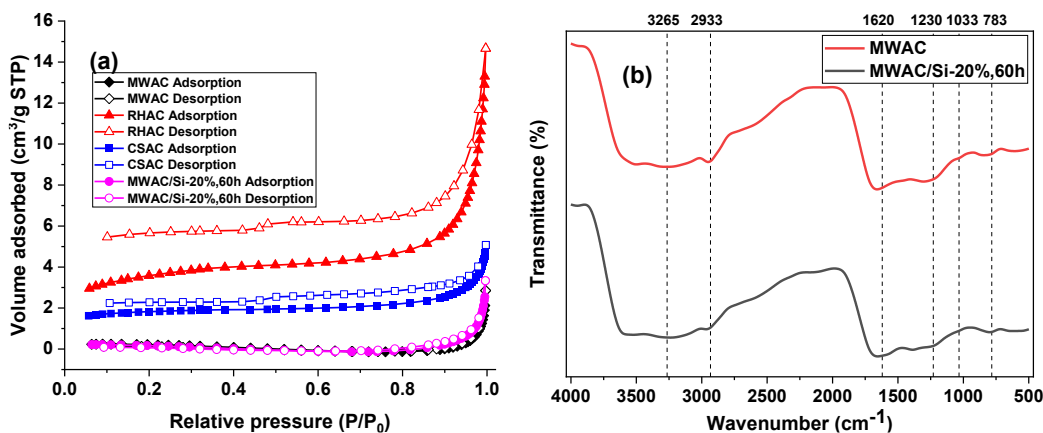


Figure 3: N_2 adsorption isotherm of different samples (a), FTIR spectra of MWAC and MWAC/Si-20%,60h (b)

Table 3: Surface area and pore parameters of different carbon samples

Sample	S_{BET} (m^2/g)	V_t (cm^3/g)	d_{avg} (nm)
MWAC	1.0133	0.003284	12.9651
RHAC	12.6385	0.020932	6.6248
CSAC	6.7532	0.007263	4.3022
MWAC/Si-20%,60h	0.3087	0.003994	51.7542

Water vapor adsorption tests on Na_2SiO_3 -impregnated biochars (19 wt%, 24 h) show that MWAC/Si-19%,24h exhibits the highest adsorption capacity compared to RHAC/Si-19%,24h and CSAC/Si-19%,24h (Figure 4). Despite having the lowest BET surface area, MWAC's hierarchical pore distribution and larger initial average pore diameter enhance water vapor accessibility. Macropores in MWAC serve as transport channels, directing water molecules into smaller pores where adsorption occurs more effectively (Gonzalez-Hourcade et al., 2022). The presence of oxygen-containing functional groups increases hydrophilicity, improving interactions with water molecules.

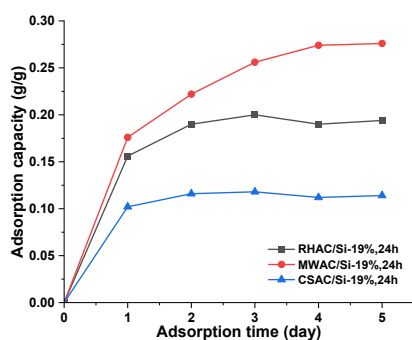


Figure 4: Water vapor adsorption capacity of different biochar desiccants

MWAC, which exhibited the highest water vapor adsorption capacity, was selected to investigate the effect of Na_2SiO_3 concentration and impregnation time. Experimental results (Figure 5(a,b)) indicate that a 20 %wt Na_2SiO_3 concentration and a 60-hour impregnation time yield the highest adsorption capacities of 0.283 g/g and 0.337 g/g, respectively. Increasing the concentration to 24 % or 27 % wt or extending the impregnation time to 72 hours reduces adsorption capacity due to pore blockage and structural alterations. Excessive silicate deposition diminishes effective surface area, while prolonged alkaline exposure may cause structural degradation, reducing adsorption efficiency. This aligns with previous findings that chemical activation requires an optimal time to balance pore formation and surface modification (Liu et al., 2024). Surface modification by Na_2SiO_3 introduces silanol and hydroxyl groups, enhancing hydrophilicity and facilitating hydrogen bonding with

water molecules, thereby improving adsorption performance. However, excessive functionalization can saturate the surface, limiting adsorption sites and altering electrostatic interactions.

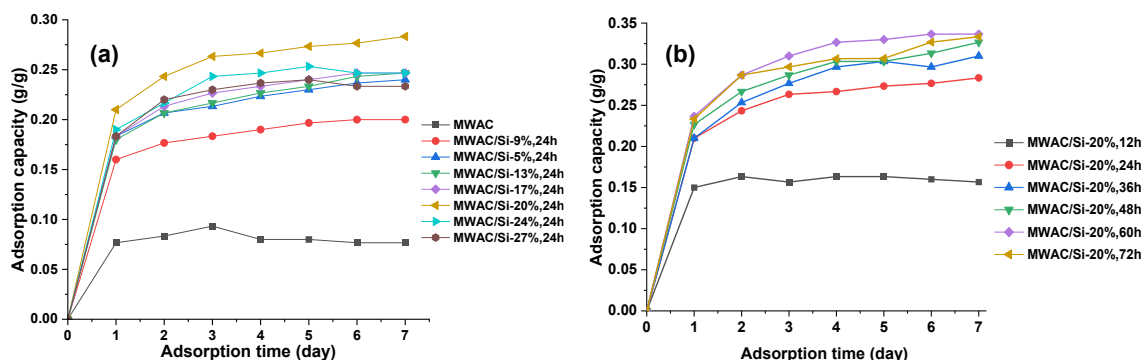


Figure 5: Adsorption capacity overtime of MWAC impregnated in (a) different Na_2SiO_3 concentration and in (b) different impregnation time

The kinetic study of different adsorbents was evaluated using linear PFO and PSO model (Table 1) resulting parameters shown in Table 4 indicates that MWAC, despite its low surface area, benefits from mesopores that enable rapid adsorption. The fitting results show R^2 values of 0.9978 (PFO) and 0.9975 (PSO), which are almost identical. Hence, no firm conclusion can be drawn regarding the dominant model for MWAC without further statistical validation. In contrast, Na_2SiO_3 -impregnated samples consistently exhibit higher R^2 for PSO than for PFO, which indicates that adsorption is better described by chemisorption involving hydrogen bonding and enhanced hydrophilicity (A'yuni et al., 2024).

Table 4: Parameters of linear PFO and PSO models adsorption curve fitting

Sample	Pseudo-first-order			Pseudo-second-order		
	k_1 (day ⁻¹)	q_e (g/g)	R^2	k_2 (g/g/day)	q_e (g/g)	R^2
RHAC/Si-19%,24h	1,7319	0,2386	0.9829	39.1176	0.2036	0.9894
MWAC/Si-19%,24h	1.1324	0.3635	0.9714	9.1912	0.2916	0.9827
CSAC/Si-19%,24h	1.6072	0.0984	0.9856	124.9055	0.1195	0.9968
MWAC	2.2174	0.0794	0.9978	414.0311	0.0833	0.9975
MWAC/Si-5%,24h	0.7571	0.1451	0.9452	24.8454	0.2028	0.9969
MWAC/Si-9%,24h	0.6571	0.1797	0.9390	15.2185	0.2444	0.9964
MWAC/Si-13%,24h	0.6651	0.2072	0.9312	12.4391	0.2521	0.9949
MWAC/Si-17%,24h	0.7653	0.1999	0.9520	14.9611	0.2536	0.9970
MWAC/Si-20%,24h	0.6551	0.1995	0.9218	13.8960	0.2883	0.9973
MWAC/Si-24%,24h	1.0087	0.2405	0.9638	17.5049	0.2599	0.9937
MWAC/Si-27%,24h	1.0239	0.2005	0.9862	23.2818	0.2457	0.9962
MWAC/Si-20%,12h	1.6770	0.1325	0.9863	121.8931	0.1683	0.9984
MWAC/Si-20%,36h	0.6770	0.2529	0.8972	9.4549	0.3184	0.9945
MWAC/Si-20%,48h	0.6389	0.2822	0.8549	8.9068	0.3324	0.9943
MWAC/Si-20%,60h	0.8385	0.2990	0.9717	9.8209	0.3491	0.9964
MWAC/Si-20%,72h	0.6617	0.2813	0.8770	9.5337	0.3385	0.9945

4. Conclusions

This study develops a sodium silicate-impregnated biochar composite with enhanced water vapor adsorption. Optimal condition was achieved with 20 wt% Na_2SiO_3 and 60 hours impregnation time yielded a maximum capacity of 0.337 g/g, four times higher than non-impregnated biochar. Despite a reduced surface area (1.0133 m^2/g to 0.3087 m^2/g) from silica deposition, the composite's hierarchical pores (average 51.75 nm diameter) and oxygen-rich functional groups significantly improved adsorption. MWAC/Si-19%,24h outperformed RHAC/Si-19%,24h and CSAC/Si-19%,24h, owing to its unique pore structure and elemental composition. Kinetic analysis revealed that MWAC gave nearly identical fits with PFO and PSO, while impregnated samples exhibited higher R^2 for PSO, indicating chemisorption associated with enhanced hydrophilicity and hydrogen bonding. The results highlight Na_2SiO_3 -impregnated biochar as a sustainable, high-performance desiccant,

combining renewable biomass utilization with superior humidity control. The work provides actionable insights for optimizing desiccants through pore engineering and chemical activation.

Acknowledgments

This research is funded by Faculty of Engineering, Dlponegoro University, contract number 035/S/Kimia/8/UN7.F3/PP/III/2025.

References

- A'yuni, D. Q., Hadianono, H., Velny, V., Subagio, A., Djaeni, M., & Mufti, N. (2024). Effect of Potassium Hydroxide Concentration and Activation Time on Rice Husk-Activated Carbon for Water Vapor Adsorption. *Iranian Journal of Materials Science and Engineering*, 21(3), 1–10. <https://doi.org/10.22068/ijmse.3522>
- A'yuni, D. Q., Subagio, A., Hadiyanto, H., Kumoro, A. C., & Djaeni, M. (2021). Microstructure silica leached by NaOH from semi-burned rice husk ash for moisture adsorbent. *Archives of Materials Science and Engineering*, 108(1), 5–15. <https://doi.org/10.5604/01.3001.0015.0248>
- Asiah, N., Djaeni, M., & Hii, C. L. (2017). Moisture Transport Mechanism and Drying Kinetic of Fresh Harvested Red Onion Bulbs under Dehumidified Air. *International Journal of Food Engineering*, 13(9), 1–8. <https://doi.org/10.1515/ijfe-2016-0401>
- Cuong, D. V., Wu, P.-C., Liu, N.-L., & Hou, C.-H. (2020). Hierarchical porous carbon derived from activated biochar as an eco- friendly electrode for the electrosorption of inorganic ions. *Separation and Purification Technology*. <https://doi.org/http://dx.doi.org/10.1016/j.seppur.2020.116813>
- Gonzalez-Hourcade, M., Reis, G. S. dos, Grimm, A., Dinh, V. M., Lima, E. C., Larsson, S. H., & Gentili, F. G. (2022). Microalgae biomass as a sustainable precursor to produce nitrogen-doped biochar for efficient removal of emerging pollutants from aqueous media Microalgae biomass as a sustainable precursor to produce nitrogen-doped biochar for efficient removal of emergi. *Journal of Cleaner Production*, 348. <https://doi.org/10.1016/j.jclepro.2022.131280>
- Guo, Y., & Wang, Q. (2023). Exploring the adsorption potential of Na₂SiO₃-activated porous carbon materials from waste bamboo biomass for ciprofloxacin rapid removal in wastewater. *Environmental Technology and Innovation*, 32. <https://doi.org/10.1016/j.eti.2023.103318>
- Jia, R.-Q., Liang, S., Xue, Z.-Y., Chu, G.-W., Zhang, L.-L., & Chen, J.-F. (2025). Reaction kinetic modeling of carbon dioxide desorption in aqueous amine solutions. *Separation and Purification Technology*, 359, 130578. <https://doi.org/https://doi.org/10.1016/j.seppur.2024.130578>
- Lee, H., Kim, H., & Kim, H. (2019). Application of Carbon Felt as a Flow Distributor for Polymer Electrolyte Membrane Fuel Cells Application of Carbon Felt as a Flow Distributor for Polymer Electrolyte Membrane Fuel Cells. *Journal of the Electrochemical Society*, 166(2), F74–F78. <https://doi.org/10.1149/2.0461902jes>
- Li, R., Shi, Y., Wu, M., Hong, S., & Wang, P. (2020). Nano Energy Improving atmospheric water production yield: Enabling multiple water harvesting cycles with nano sorbent. *Nano Energy*, 67, 104255. <https://doi.org/https://doi.org/10.1016/j.nanoen.2019.104255>
- Liu, S., Wu, P., Fu, G., Zhang, S., Yang, Y., Huai, X., & Xu, M. (2024). Characterization of Water Vapor Sorption Performance and HeatStorage of MIL-101 (Cr) Complex MgCl₂, LiCl LaCl₃ System for Adsorptive Thermal Conversion. *ACS Omega*, 9(1), 509–519. <https://doi.org/10.1021/acsomega.3c06004>
- Mongkito, V. H. R., Anas, M., Erniwati, Rusman, L. O., & Anjanihu, H. (2020). Technology of Carbon : Effect of Activation Temperature on Characterization the Ultimate and Proximate Activated Carbon of Palm Bunches (Arenga Pinnata (Wurmb). Merr). *International Journal of Innovative Technology and Exploring Engineering*, 9(4), 1268–1274. <https://doi.org/10.35940/ijitee.D1366.029420>
- Nandiyanto, A. B. D., Oktiani, R., & Ragadhita, R. (2019). How to Read and Interpret FTIR Spectroscopy of Organic Material. *Indonesian Journal of Science and Technology*, 4(1), 97–118. <https://doi.org/10.17509/ijost.v4i1.15806>
- Thommes, M., Kaneko, K., Neimark, A. V., Olivier, J. P., Rodriguez-Reinoso, F., Rouquerol, J., & Sing, K. S. W. (2015). Physisorption of gases, with special reference to the evaluation of surface area and pore size distribution (IUPAC Technical Report). *Pure and Applied Chemistry*, 87(9–10), 1051–1069. <https://doi.org/10.1515/pac-2014-1117>
- Vivekh, P., Islam, M. R., & Chua, K. J. (2020). Experimental performance evaluation of a composite superabsorbent polymer coated heat exchanger based air dehumidification system. *Applied Energy*, 260(March 2019). <https://doi.org/10.1016/j.apenergy.2019.114256>
- Wang, C., Yang, B., Ji, X., Zhang, R., & Wu, H. (2022). Study on activated carbon/silica gel/lithium chloride composite desiccant for solid dehumidification. *Energy*, 251. <https://doi.org/10.1016/j.energy.2022.123874>
- Wolkoff, P. (2018). Indoor air humidity, air quality, and health – An overview. *International Journal of Hygiene and Environmental Health*, 221(3), 376–390. <https://doi.org/10.1016/j.ijheh.2018.01.015>